Bioorganic Chemistry 86 (2019) 538–549

Contents lists available at ScienceDirect

Bioorganic Chemistry

journal homepage: www.elsevier.com/locate/bioorg

Identification of a new tamoxifen-xanthene hybrid as pro-apoptotic anticancer agent

Elena Catanzaro[a], Francesca Seghetti[b], Cinzia Calcabrini[a], Angela Rampa[b], Silvia Gobbi[b], Piero Sestili[c], Eleonora Turrini[a], Francesca Maffei[a], Patrizia Hrelia[d], Alessandra Bisi[b], Federica Belluti[b,*,1], Carmela Fimognari[a,*,1]

[a] Department for Life Quality Studies, Alma Mater Studiorum-University of Bologna, Corso d'Augusto 237, 47921 Rimini, Italy
[b] Department of Pharmacy and Biotechnology, Alma Mater Studiorum-University of Bologna, Via Belmeloro 6, 40126 Bologna, Italy
[c] Department of Biomolecular Sciences, University of Urbino Carlo Bo, Via I Maggetti 26, 61029 Urbino (PU), Italy
[d] Department of Pharmacy and Biotechnology, Alma Mater Studiorum-University of Bologna, Via Irnerio 48, 40126 Bologna, Italy

ARTICLE INFO

Keywords:
apoptosis
Bax, Bcl-2, breast cancer
genotoxicity
γ-H2A.X phosphorylation, PARP cleavage, tamoxifen
triphenylethylene
xanthene scaffold

ABSTRACT

Breast cancer is the most diagnosed type of cancer among women for which an exhaustive cure has not been discovered yet. Nowadays, tamoxifen still represents the gold standard for breast cancer therapy; it acts on both estrogen receptor-positive and estrogen receptor-negative breast cancers. Unfortunately, its toxicity and the related chemoresistance undermine its antitumor potential. In this paper, new tamoxifen-based derivatives with a rigid structural motif in their structure were designed, synthesized, and evaluated to assess their antitumor behavior. All the tested compounds affected estrogen receptor-positive tumor (MCF-7) cell growth, even with different extents, among which, the most active ones proved also to induce mitochondria-mediated apoptosis through activation of PARP cleavage, decrease in Bax/Bcl-2 ratio and increase in Bim gene expression levels. Here we found that the compound **1**, carrying a rigid xanthene core, turned out to be the most promising of the set showing an activity profile comparable to that of tamoxifen. Furthermore, a more favorable genotoxic profile than tamoxifen made compound **1** a promising candidate for further studies.

1. Introduction

Cancer, among the non-communicable diseases, is the second leading cause of death. It is responsible for an estimated 18.1 million new cases and 9.6 million cancer deaths in 2018 [1]. Moreover, among the various cancer subtypes, breast cancer is the second most reported malignancy and the first within women with 2.09 million cases; 1 out of 4 women was diagnosed with breast cancer, with a survival rate greater than 85% [2,3]. Indeed, improvements in prevention, early detection and innovative treatment approaches have significantly increased the number of positive outcomes, even if the heterogeneity of the disease and the limitations of current treatments still make breast cancer a significant concern for public health. Antitumor therapeutics often exert their effects by inducing apoptosis in cancer cells [4].

Apoptosis, or programmed cell death, is an essential, evolutionarily conserved process that exerts an essential influence in development, homeostasis, but also in carcinogenesis of mammary gland cells. It is carried out by caspases, which are known to be activated mainly by the extrinsic and/or the intrinsic pathway. The first of these involves the interaction of a death receptor, a cell surface transmembrane receptor with specific protein ligands, while the second is triggered in response to DNA damage and depends on the involvement of mitochondria. Recent outcomes pointed out to a link between the extrinsic and intrinsic pathways, providing support to the concept of converging instead of distinct routes [5]. Bcl-2 family of proteins controls the intrinsic apoptotic pathway and is composed by the anti-apoptotic 'guardian' proteins, among which BCL-2 is responsible for programmed cell death evasion, the pro-apoptotic 'effectors' BAX and BAK, and the BH3-only 'sensor' proteins. Approximately 75% of primary breast cancers express high levels of BCL-2, with a prevalence in ER-positive tumors (85% overexpression). Thus, downregulation of BCL-2 expression can be regarded as a novel and promising anticancer strategy.

Abbreviations: ER, estrogen receptor; FCC, flash column chromatography; i.m., isomers mixture; PARP, poly (ADP-ribose) polymerase-1; SERM, selective estrogen receptor modulator; TAM, tamoxifen

* Corresponding authors.
E-mail addresses: federica.belluti@unibo.it (F. Belluti), carmela.fimognari@unibo.it (C. Fimognari).
[1] These authors contributed equally to this work.

https://doi.org/10.1016/j.bioorg.2019.02.017
Received 24 September 2018; Received in revised form 18 January 2019; Accepted 6 February 2019
Available online 10 February 2019
0045-2068/ © 2019 Published by Elsevier Inc.

Tamoxifen (*Z*-1-{4-[2-(dimethylamino)ethoxy]phenyl}-1,2-diphenyl-1-butene, TAM), is a first-generation selective estrogen receptor (ER) modulator widely used in the treatment of both advanced and early-stage breast cancer [6]. Since its approval in 1977, it has remained the gold standard for hormonal therapy [7], and in 1998 its use has been also approved to lower the incidence of breast cancer for both pre- and post-menopausal women at "elevated risk" [8]. Noteworthy, in post-menopausal women its use is controversial, as a number of side effects, including an increased occurrence of endometrial carcinomas, have been reported [7,9], mainly due to its metabolic conversion to reactive intermediates such as 4-hydroxy-TAM [10] or α-hydroxy-TAM [11]. Besides, intrinsic or acquired drug resistance can significantly reduce TAM therapeutic efficacy, leading to recurrences [12].

Interestingly, TAM efficacy in ER-negative malignancies has been also reported [8,13], leading to speculate on an ER-independent anticancer mechanism, that clearly widens the therapeutic potential of this drug. A number of studies confirmed the modulation of different signaling proteins and the induction of distinctive cellular morphological modifications consistent with an induction of apoptosis. In this respect, both the extrinsic and intrinsic pathways are involved, with the activation of caspases -8, -9, -3 and PARP [14] and the modulation of oncoproteins belonging to the BCL-2 family [15], respectively.

Extensive medicinal chemistry efforts have been devoted at developing novel TAM-based analogues, with reduced side effects, and with increased effectiveness, by modifying the *trans*-triphenylethylene (TPE) framework. [16] A number of derivatives endowed with expanded biological activities have been developed by means of the hybridization approach [17,18].

In this scenario, aimed at identifying new lead-like molecules that would serve as chemical platform to be further modified in order to elucidate the mechanism underlying TAM biological effect, some established medicinal chemistry design strategies were applied to create a small set of structurally different TPE-based analogues. In particular: 1) conformational restriction and 2) scaffold decoration approaches were pursued. As depicted in Fig. 1, to reduce the flexibility: 1-a) the TPE core was merged with a xanthene moiety to obtain the compound **1**; 1-b) an aminobutinyloxy side chain, instead of the aminoethoxy, was introduced (**2**–**3**); in this set, the importance of the *trans*-TPE configuration with respect to the *cis* was also evaluated (**2** *vs* **2a**). Moreover, properly selected substituents were incorporated on the TPE scaffold:2-a) to mimic the active metabolite 4-OHTAM, the 4-hydroxylated analogue of **3** was also synthesized (**4**); 2-b) the TPE nucleus was decorated with fluorine atoms (compound **5**), since fluorinated compounds often have more favorable pKa and lipophylicity that may be useful in enhancing therapeutic efficacy [19].

As regards the amino functions, cyclic amines were preferentially introduced, as they are known to maintain the activity of the dimethylamino moiety, while being subjected to a more favorable metabolic fate [20,21].

The newly synthesized compounds **1**–**5** were tested to evaluate their antitumor profile in terms of cytotoxicity and pro-apoptotic potential.

2. Results and discussion

2.1. Compounds synthesis

As traditionally reported for TAM-related compounds, in this paper *trans* and *cis* are used to designate the relative positions of the ethyl group on the olefinic bond and the aryl ring bearing the 4-alkoxyamino function (A_2B_2). Whether a compound of given configuration by this nomenclature is *Z* or *E* depends on the nature of the 4-substituent [21]. Our attention was mainly focused on obtaining the *trans* isomers, due to the structural analogy with TAM.

The desired isomers (intermediates **7**, **13**, **13a**, **14**, and **15**) were obtained in a good grade of purity by following different strategies: fractioned crystallization by suitable solvent (**14**) or flash column chromatography (FCC), upon previous transformation into the corresponding perfluorotolyl ether derivative (**7**, **13**, **13a**, and **15**), as

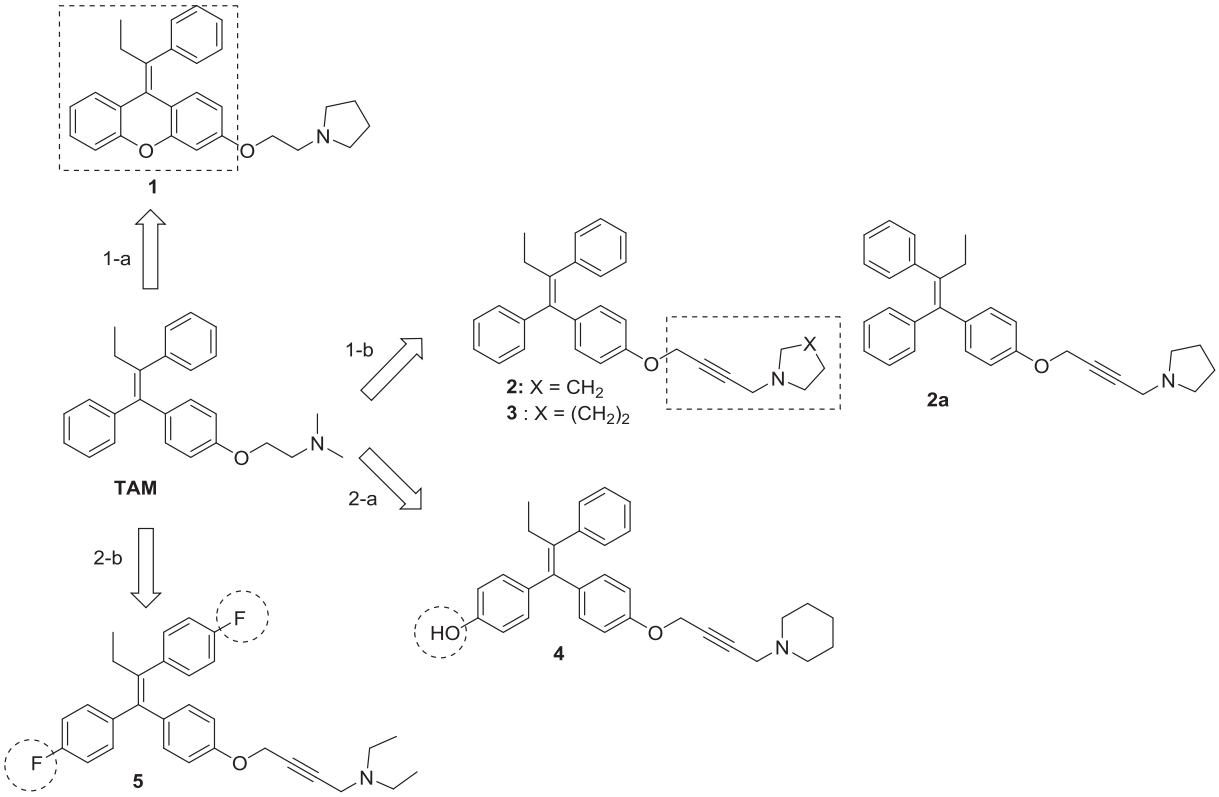

Fig. 1. Structure of TAM and design overview of the newly synthesized analogues (**1**–**5** and **2a**).

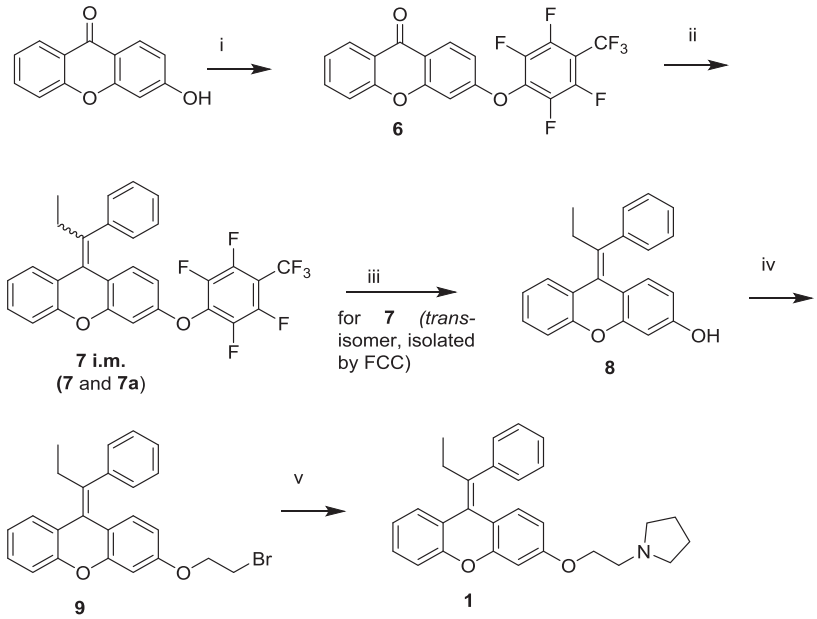

Reagents and conditions: i) $C_6F_5CF_3$, NaOH (aqueous), $(nBu)_4N^+HSO_4^-$, DCM, 1M NaOH; ii) propiophenone, $TiCl_4$, Zn, THF, -15 °C-reflux; iii) $NaOCH_3$, DMF, r.t.; iv) 1,2-dibromoethane, K_2CO_3, acetone, r.t.; v) pirrolidine, Et_3N, THF, r.t.

Scheme 1. Synthetic strategy for compound **1**.

already reported [22]. The *cis*-isomers, as mentioned above, were labeled with the "a" letter after the compound number.

As depicted in Scheme 1, 3-hydroxy-9*H*-xanthen-9-one was reacted with octafluotoluene, using a phase transfer catalyst, to obtain intermediate **6**, that was then coupled with propiophenone under the McMurry reaction conditions [23] affording **7 i.m.** (isomer mixture) of compounds **7** (isomer *Z*, or *trans*) and **7a** (isomer *E*, or *cis*). This was then subjected to FCC to obtain the desired *trans* isomer **7**. The perfluorotolyl protecting group was removed by treatment with NaOMe to give the phenol **8**, that was then alkylated with 1,2-dibromoethane, in acetone and in the presence of K_2CO_3, affording **9**. Finally, it was reacted with pyrrolidine, at room temperature and in the dark (to avoid *cis-trans* isomerization), to give the desired compound **1**. Scheme 2 reports the synthetic strategy to obtain the TPE-based phenols (**13**, **13a**, **14**, and **15**) as pure isomers. In detail, 4-fluorophenyl-4-hydroxyphenylmethanone **11** and 4-fluoropropiophenone were reacted under the McMurry reaction conditions to give **14 i.m.**; fractionated crystallization from isopropanol allowed isolating the pure *trans* isomer **14**. Conversely, reaction of (4-hydroxyphenyl)(phenyl)methanone **10** and (4-hydroxyphenyl)(4-methoxyphenyl)methanone **12** with propiophenone gave **13 i.m.** and **15 i.m.**, respectively. Then, **13 i.m.** and **15 i.m.** were converted into the corresponding perfluorotolyl ethers **16 i.m.** and **17 i.m.**, respectively, that were subjected to FCC to obtain the desired pure isomers: **16** (*Z*), **16a** (*E*), and **17** (*Z*). The perfluorotolyl function was then removed to achieve the desired hydroxy derivatives **13**, **13a** and **15**, that were reacted with propargyl bomide, under the classic Williamson reaction conditions (Scheme 3) to obtain **18** (*Z*), **18a** (*E*), **19** and **20**. Finally, the Mannich reaction, in the presence of formaldehyde, the selected amine, and $CuSO_4$ as catalyst, afforded the desired compounds **2** (*Z*), **2a** (*E*), **3**, **5**, and **21**, whose methoxy group was then cleaved by treatment with BBr_3 affording compound **4**.

The configuration of the synthetized molecules was readily assigned by ^{1}H NMR spectroscopy following relative positions of the aryl proton signals arising from the A_2B_2 system of the 4-substituted phenyl ring and/or the OCH_2 signal arising from the side chain. In particular, in the *trans* isomer the above signals are considerably upfield in comparison to those of the corresponding *cis* isomer [24]. Similarly, the proton signals of the basic side chain resonate at a lower frequency in the *trans*-isomer, with respect to the corresponding *cis*-isomer [24–26]. 1D-NOESY experiments were also performed on **1** and **18** to further confirm the configuration assignment (See supporting information Figs. S5 and S7, respectively).

2.2. Cytotoxic activity

Firstly, the newly synthesized derivatives **1**–**5** were evaluated for their antitumor potential on ER-positive breast cancer cell line (MCF-7) in comparison to TAM (Table 1). Cell viability after 24 h treatment, determined by MTT assay, was effectively decreased by analogues **1**, **2**, and **3** in a dose-dependent manner. In particular, at the highest tested concentration of 40 μM compound **1**, like TAM, killed almost all cells. Derivatives **2**, **2a** and **3** appreciably modulated cell viability at the concentrations of 20 and 40 μM reaching a plateau. On the contrary, derivative **4** and **5** significantly decreased MCF-7 cell viability only at the highest concentration of 40 μM (Fig. S1). Definitively, the xanthene-based hybrid, **1** turned out to be the most active compound in this set, showing an IC_{50} value comparable to that of TAM (12.4 μM and 10.4 μM, respectively). A slightly decreased potency was observed for analogues **2** and **3**, bearing a rigid butinyl side chain, that maintained a two-digit micromolar potency (IC_{50s} = 20.7 and 19.3 μM, respectively). As expected, for the corresponding *cis*-isomer **2a**, a further drop in potency was recorded. Finally, the decoration of the TPE scaffold with an OH group (**4**) or fluorine atoms (**5**) proved to be detrimental (IC_{50} values around 40 μM).

To assess whether the cytotoxic activity was dependent on ERs, the most promising derivative **1** was selected to be evaluated on the MDA-MB-231 ER-negative cell line. In particular, at 40 μM, the percentages of viable cells were 18 and 25 (Fig. S2) for **1** and TAM, respectively. A remarkable antiproliferative effect, comparable to that of TAM, was thus observed, with IC_{50} values of 25.4 and 28.9 μM, respectively

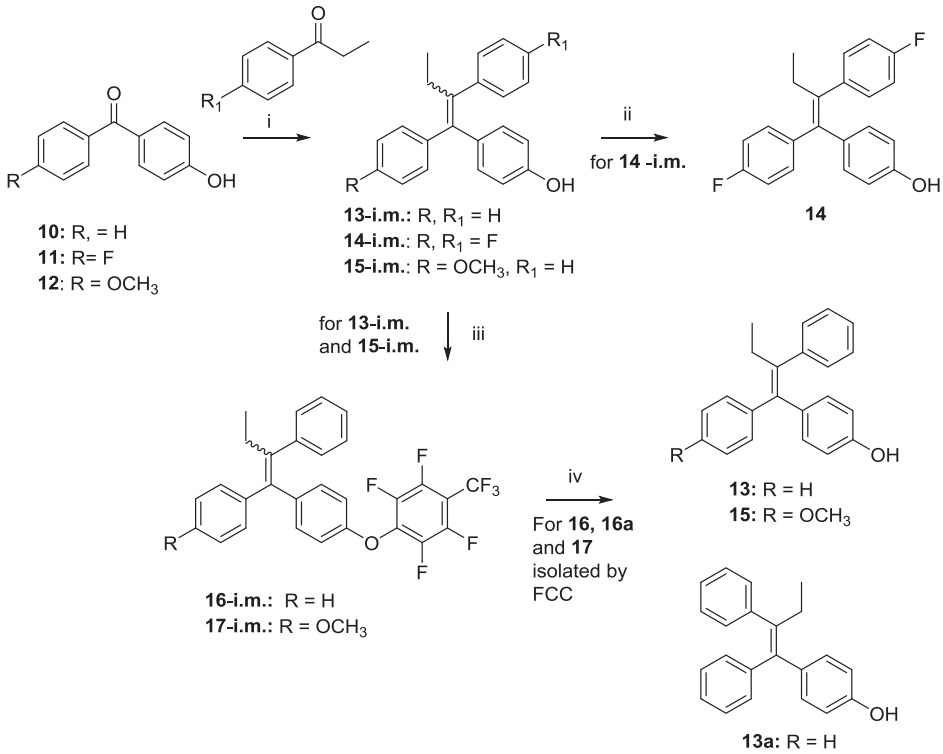

Reagents and conditions: i) selected propiophenone, $TiCl_4$, Zn, THF, -15 °C-reflux; ii) fractioned crystallization; iii) $C_6F_5CF_3$, $(nBu)_4N^+HSO_4^-$, DCM, 1M NaOH; iv), $NaOCH_3$, DMF r.t.

Scheme 2. Synthetic strategy for TPE-based synthons (**12**, **12a**, **13**, **14**).

(Table 1). The low efficacy of TAM on ER-negative tumors [27] was confirmed in our experimental settings: in this cell line TAM's IC_{50} was about three times higher than that observed in MCF-7 cells. A similar but less marked trend was observed for **1**, whose IC_{50} on MDA-MB-231 cells was about twice as high as that observed on ER-positive cells. The comparable behavior of TAM and **1** on both ER-positive and -negative cell lines might likely suggest their capability to modulate some ER-independent pathways.

From these data some considerations could be drawn: -a) the introduction of a rigid motif on the TAM side chain proved to slightly

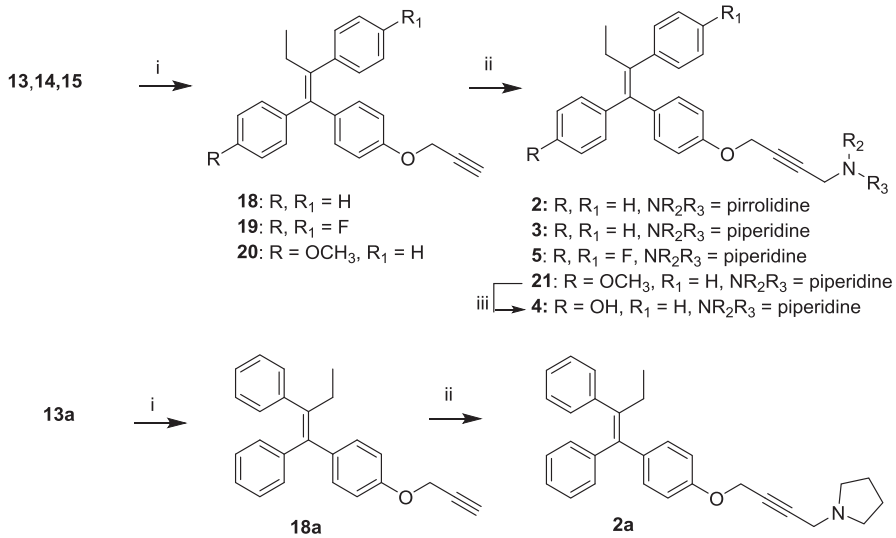

Reagents and conditions: i) 3-bromoprop-1-yne, K_2CO_3, acetone, reflux; ii) HCHO, $CuSO_4$, selected amine; iii) BBr_3, DCM, -78 °C-r.t.

Scheme 3. Synthetic strategy for tested compounds **2**, **2a**, **3**–**5**.

Table 1
Cytotoxic activities of TAM-based derivatives (**1**–**5**) and tamoxifen (TAM).

Comp	Structure	ER-positive MCF-7 IC_{50} (μM)[a]	ER-negative MDA-MB-231
1	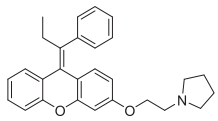	12.4 ± 0.54	25.4 ± 0.40
2	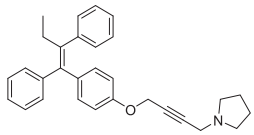	20.7 ± 4.05	n.d.
2a	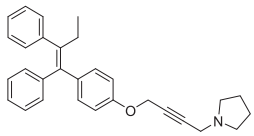	31.3 ± 2.90	n.d.
3	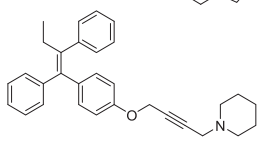	19.3 ± 2.22	n.d.
4	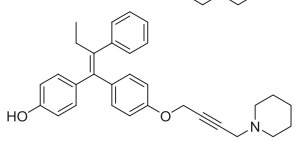	39.70 ± 3.59	n.d.
5	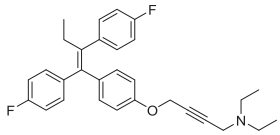	40.81 ± 3.02	n.d.
TAM	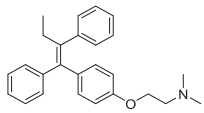	10.5 ± 0.76	28.9 ± 1.35

[a] IC_{50} values were obtained after 24 h treatment of MCF-7 or MDA-MB-231 cell lines; n.d.: not determined.

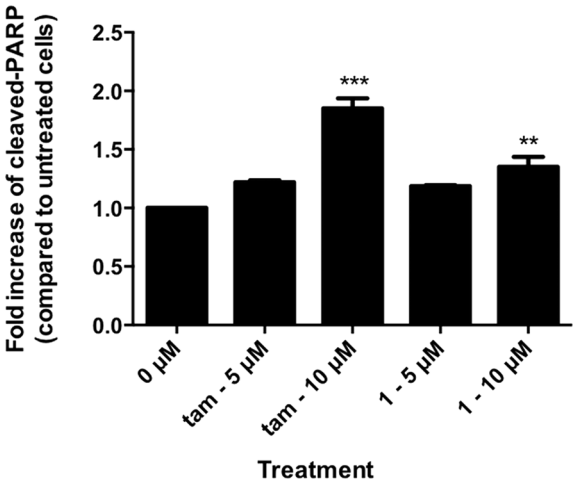

Fig. 2. Fold-increase of cleaved PARP compared to untreated cells after 24 h treatment of MCF-7 cells with TAM or **1**. Cleavage of PARP was determined by flow cytometry using an antibody specific for the 85 kDa PARP cleaved portion. The bars represent the mean values of four experiments ± *SEM*; the significance level compared to the control was specified as $p < 0.01$ (**), $p < 0.001$ (***) using one way ANOVA and the Dunnett's multiple comparison test.

decrease the antiproliferative effect on ER-positive cells, as in compounds **2** and **3**; b) as already known for TAM-related compounds, the nature of the amino function did not play a pivotal role for cytotoxicity; c) the insertion of a hydroxy group on the main scaffold of **3**, as in analogue **4**, induced a further drop in potency; d) the di-fluorinated TPE substitution pattern proved to negatively affect the cytotoxic profile (**5**); e) the locked TPE scaffold obtained by its hybridization with a xanthene core, allowed to retain an appreciable anticancer activity (compound **1**).

2.3. Apoptosis studies

To get insight into the molecular basis of the cytotoxic activity of the most interesting TAM-based derivatives (**1**, **2** and **3**) apoptosis studies, on MCF-7 cell line, were performed. In particular, the underlying mechanisms of the apoptotic event, by evaluating the mRNA levels and/or protein expression of PARP, Bax, Bcl-2, p53, and Bim, key mediators involved in the execution of this process, were explored.

PARP is an indicator of DNA single strand break and one of the most important reporters of caspase-3 activation. During the early stages of apoptosis, activated-caspase-3 cleaves PARP in two fragments, leading to DNA binding and interfering with DNA repair enzymes [28]. All the analyzed derivatives induced PARP cleavage to a different extent (data not shown), being compound **1** the most effective, showing a behavior comparable to TAM. At the highest tested concentration (10 μM), TAM and **1** induced a 1.85 and 1.35 fold increase in cleaved PARP, respectively, *versus* non-treated cells (Fig. 2). As also observed in the

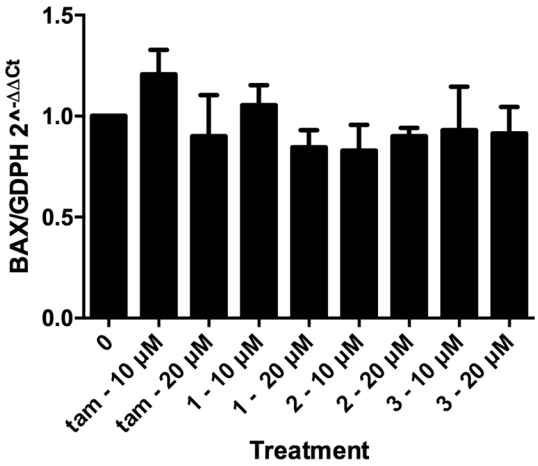

Fig. 3. Effect of TAM, **1**, **2** and **3** on Bax gene expression compared to untreated cells after 24 h treatment of MCF-7. Bax gene expression was determined by real time PCR. Differences in mRNA expression are reported as value ± *SEM* and represent the relative expression calculated through the $2^{-\Delta\Delta Ct}$ method. The bars represent the mean values of four experiments ± *SEM*.

cytotoxicity studies, the xanthene derivative **1** again proved to be slightly less active with respect to TAM.

Bcl-2 and Bax are homologous proteins that play a central role in inducing mitochondrial apoptosis: while Bcl-2 is an ubiquitous inhibitor of apoptosis, Bax is a promoter of cell death by inhibiting the pro-survival role of Bcl-2. Treatment of MCF-7 cells with the selected compounds did not affect Bax gene expression as shown in Fig. 3.

In the same experimental conditions, an overall decrease in Bcl-2 protein and mRNA levels was observed for all tested derivatives. Also in this context, **1** proved to be the most potent inhibitor of the series as, at 10 μM concentration, it elicited effects comparable to those observed for TAM treatment. To obtain the same effect, a double concentration was required for derivatives **2** and **3** (Fig. 4).

Due to the opposite effects of Bax and Bcl-2, the Bax/Bcl-2 ratio correlates with the propensity of a cell to undergo apoptosis and may be helpful in predicting clinical outcome [29]. In this respect, for all tested derivatived an increase of Bax/Bcl-2 ratio was noticed suggesting their feasibility to circumvent cancer cells apoptosis deficiency by affecting tumor progression and aggressiveness.

P53 is a tumor suppressor gene that plays a key role in cell cycle progression and apoptosis and, among other mechanisms, has been shown to act through Bcl-2-silencing [30]. It is mutated in more than 50% of tumors [31] but, despite this high susceptibility and frequency, only 20–30% of breast cancers (and most ER-negative tumors) are characterized by this mutation [32]. Several studies have been performed to elucidate the mechanism underlying Bcl-2 expression in ER-positive cell lines and whether its downregulation is associated with p53 intervention [33]. Different results were found in literature: in 1994, Haldar and colleagues [30] reported a possible role of wild-type p53 in TAM-induced apoptosis and an association with Bcl-2 expression, whereas in 1998 Fattman and colleagues [29] and Zhang et al. in 1999 [33] proposed a p53-independent pathway.

The results obtained with the new derivatives agreed with this latter hypothesis, since no variation in p53 gene or protein expression has been registered (data not shown), leading to speculate that Bcl-2 downregulation is independent of a modulation at the transcriptional level of p53. However, considering that some recent studies showed that p53 interacts with ER and that such functional interaction results in the suppression of the p53-mediated apoptotic response [34], the employment of an ER-positive cell line in this study could be responsible for the lack of p53 overexpression observed after TAM and TAM-analogues treatments.

To deeply investigate the mechanism responsible for the antitumor effect of derivatives **1**–**3**, the involvement of Bim was also studied. This 'BH3-only' subclass of pro-apoptotic proteins, intrinsically responsible for the initiation of apoptosis, is also a cytoskeletal integrity sensor. It represents a key factor in mitochondria-mediated apoptosis since it interacts with Bax and causes the release of apoptogenic factors that in turn activate caspase-3 [35]. We therefore evaluated whether Bim expression was upregulated in response to treatment with the selected compounds. As depicted in Fig. 5, the tested compounds determine an increase in Bim gene expression levels, leading to speculate on a involvement of 'BH3-only' in regulating mitochondria-mediated apoptosis of the newly synthetized TAM-based analogues **1**–**3**. However, TAM shows a concentration-dependent trend on BIM modulation, while compounds **1**, **2** and **3** promoted it in a different course. The effect of compound **2** at 10 μM was not statistically different to the effect of the same compound at 20 μM. The same applies for compound **3**. The low modulation of BIM could reflect the poor cytotoxic potential of compounds **2** and **3** compared to that of TAM, while a different mechanism of action could characterize compound **1**. Indeed, compound **1** showed another different trend. At 10 μM it upregulated BIM at least doubling its physiological levels, while at the highest tested concentration it didn't modulate it. BIM has been targeted as a critical protein for TAM mechanism of action. As an example, the downregulation of this protein is one of the causes of TAM resistance [36]. To understand compound **1** mechanism of action, further studies will be needed. For instance, it would be worth evaluating the modulation of Forkhead box, class O 3a (foxO3a) by compound **1**. In fact, FoxO3a is accountable for the transcriptional up-regulation of BIM that promotes apoptosis of breast cancer cells mediated by TAM [37]

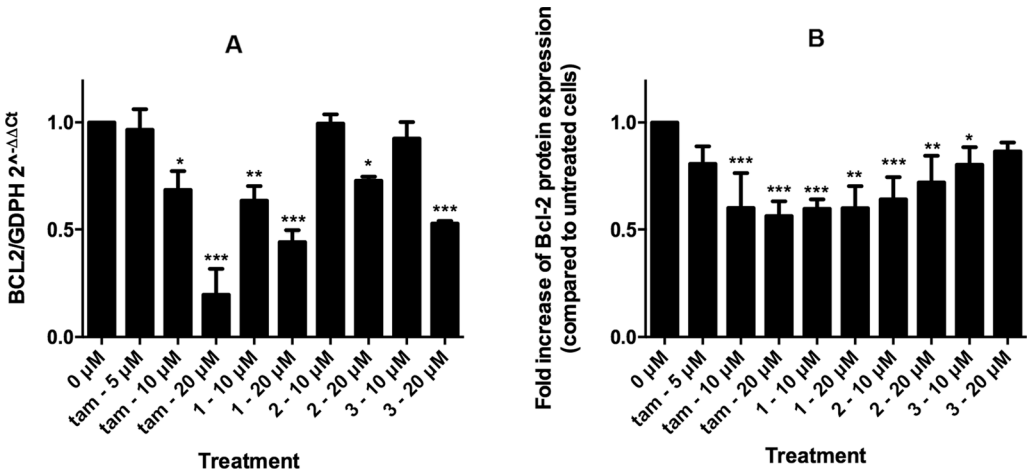

Fig. 4. Effect of **TAM**, **1**, **2** and **3** on Bcl-2 expression (A. gene or B. protein) compared to untreated cells after 24 h treatment of MCF-7. A. Bcl-2 gene expression was determined by real time PCR. Differences in mRNA expression are reported as value ± *SEM* and represent the relative expression calculated through the $2^{-\Delta\Delta Ct}$ method. B. Bcl-2 protein expression was determined by flow cytometry using a specific antibody. The bars represent the mean values of four experiments ± *SEM*; the significance level compared to the control was specified as $p < 0.05$ (*), $p < 0.01$ (**), $p < 0.001$ (***) using one way ANOVA and the Dunnett's multiple comparison test.

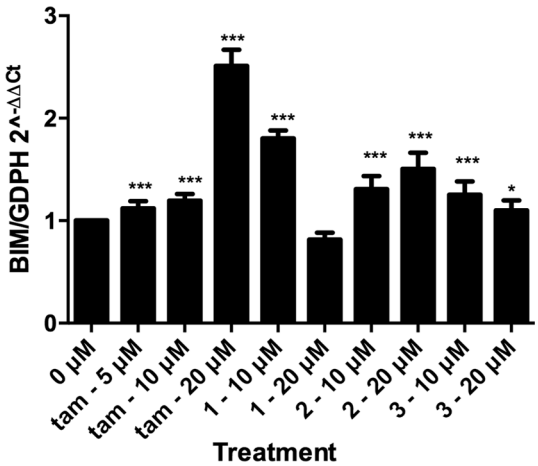

Fig. 5. Effect of **TAM**, **1**, **2** and **3** on Bim gene expression compared to untreated cells after 24 h treatment of MCF-7 cells. Bim gene expression was determined by real time PCR. Differences in mRNA expression are reported as value ± *SEM* and represent the relative expression calculated through the $2^{-\Delta\Delta Ct}$ method. The bars represent the mean values of four experiments ± *SEM*; the significance level compared to the control was specified as $p < 0.05$ (*), $p < 0.001$ (***) using one way ANOVA and the Dunnett's multiple comparison test.

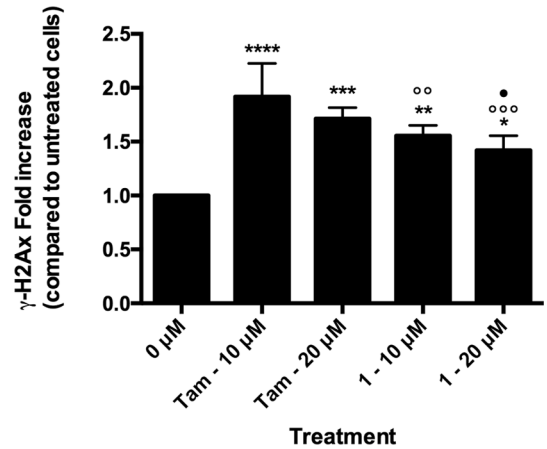

Fig. 6. Phosphorylation of histone (γ-H2A.X) induced by **TAM** or **1** in MCF-7 cells after 6 h treatment. Histone phosphorylation was analyzed by flow cytometry using an anti-γ-H2A.X-Alexa Fluor® antibody. The bars represent the mean values of four experiments ± SEM; the significance level compared to the control was specified as $p < 0.05$ (*), $p < 0.01$ (**), $p < 0.001$ (***), $p < 0.0001$ (****); compared to TAM 10 μM as $p < 0.01$ (°°), $p < 0.001$ (°°°); and compared to TAM 20 μM as $p < 0.05$ (•).

In summary, the results suggest that compounds **1**–**3**, similarly to TAM, trigger apoptosis *via* an appropriate balance between pro-apoptotic and pro-survival proteins.

Among the tested compounds, the xanthene-TAM hybrid **1**, showed the most promising anticancer effects.

2.4. Genotoxicity

In order to elaborate a preliminary risk/benefit profile, the genotoxicity of **1**, the most promising compound of this series, was investigated in Jurkat cells in comparison to TAM. DNA damage was assessed through the quantification of histone H2A.X (γ-H2A.X) phosphorylation, a biomarker of double-strand DNA breaks. Histone phosphorylation provides a good indication of the ability of a xenobiotic to interact with DNA and cause pre-mutational lesions, *i.e.* repairable *per se*. After 6 h, at 10 or 20 μM treatment with **1**, Jurkat cells showed a 1.4- and 1.2-fold increase in the phosphorylation of γ-H2A.X, respectively, compared to non-treated cells. Under the same conditions, TAM induced an increase of 1.7 and 1.5, respectively (Fig. 6).

The quantitative differences in DNA damage may lie in different metabolic processes that the two molecules are subjected to [38]. Indeed, TAM bio-activation involves the production of metabolites, namely a carbocation [39], *ortho*-quinone [40] and/or quinone methide [41] able to induce DNA damage, both directly through the formation of adducts, and/or indirectly, by increasing ROS levels. Several studies reported the mutagenicity of TAM and its ability to induce micronuclei formation in metabolically competent human cells [42,43]. The peculiar structural features of **1**, in particular the presence of the oxygenated scaffold and the cyclic amino function in the side chain, could favorably affect its metabolic fate, reducing this well-known TAM's drawback.

3. Conclusions

A small series of TPE-based derivatives was designed, synthesized and tested to evaluate their anticancer potential. Some structural modifications were performed in order to reduce the flexibility of different peculiar TAM fragments *i.e.* the aminoethoxy side chain and the TPE core. All the newly synthesized compounds were able to inhibit the proliferation of the ER-positive breast cancer cell line MCF-7, even if to a different extent. The TPE-based analogs bearing a rigid butinyl side chain (**2**, **2a**, **3** and **4**) turned out to be less active than TAM, while the TPE-constrained compound **1** proved to maintain the same range of activity and emerged as the most potent of the series, maintaining an appreciable activity in ER-negative MDA-MB-231 cell line as well. In particular, while TAM was significantly more active on ER-positive with respect to ER-negative cells (IC_{50} values of 10.5 and 28.9, respectively), only a two-fold drop in potency shifting from ER-positive to ER-negative cells was observed for compound **1** (IC_{50} values of 12.4 and 25.4, respectively). This trend suggests that **1** could exert its cytotoxic effect involving some ER-independent pathways. Particular attention was given at elucidating the molecular basis of the pro-apoptotic behavior (**1**, **2** and **3**) on MCF7 cells. The recruitment of caspase-3, confirmed by the activation of PARP cleavage, was induced by all derivatives, being **1** the most active. Moreover, a downregulation of the antiapoptotic guardian Bcl-2 gene expression was also observed for all compounds, again particularly pronounced for **1**. This analogue also proved to modulate Bim gene expression levels, providing evidence that the induction of apoptosis is a pivotal mechanism by which compound **1** exert its anticancer effect. Moreover, a more favorable genotoxic profile was observed for this compound with respect to TAM, pinpointing this new molecule as a promising lead compound, worth to be further studied and optimized. In particular, further carefully designed studies on normal non-transformed cells are necessary to evaluate whether compound **1** has a selective activity for cancer cells and to better understand its toxicological profile.

4. Experimental section

4.1. Synthesis

Starting materials, unless otherwise specified in the Experimental Section, were used as high-grade commercial products. Solvents were of analytical grade. Melting points were determined in open glass capillaries, using a Büchi apparatus and are uncorrected. NMR spectra were recorded on a Varian Gemini spectrometer at 400 MHz (^{1}H), 100 MHz (^{13}C), and 376 MHz (^{19}F). Unless otherwise indicated $CDCl_3$ was used as a solvent and tetramethylsilane (TMS) as an internal standard. Chemical shifts (δ) were reported as parts per million (ppm value) and standard abbreviations, indicating spin multiplicities, were given as follow: s (singlet), d (doublet), t (triplet), br (broad), q (quartet) or m (multiplet). Mass spectra were recorded on a Waters ZQ 4000 apparatus

operating in electrospray mode (ES). Reactions were followed by thin layer chromatography (TLC) on precoated silica gel plates (Merck Silica Gel 60 F254) and then visualized with a UV lamp. Purification of synthesized compounds was carried out by flash column chromatography (FCC) using 100–200 mesh (Merck) silica gel as stationary phase. The purity of the tested compounds was determined by HPLC analysis. The analyses were performed under direct phase conditions on a Phenomenex Lux 5u cellulose column (250 × 4.60 mm), by using a ternary mixture of *n*-hexane/*i*-PrOH/DEA 90:9.99:0.1 as mobile phase, flow rate: 0.8–1.0 mL/min, the injection volume was 5 μL and peaks were detected at 254 nm. All tested compounds were found to have > 5% purity. Compounds were named using Chem-BioDraw Ultra 14.0 IUPAC name algorithm developed by CambridgeSoft Corporation.

4.1.1. General procedure for the synthesis of the perfluorotolyl ethers (6, 16 i.m., 17 i.m.).

A mixture of phenol derivative (1.0 eq), octafluorotoluene (1.0 eq), tetrabutylammonium hydrogen sulfate (TBAHS, 0.5 eq) in DCM (10 mL/mmol) and 1.0 M NaOH (10 mL/mmol) was stirred at room temperature for 1 h. The organic phase was separated, dried over Na_2SO_4, and the solvent was removed under reduced pressure to give a crude product, which was subjected to FCC purification using a suitable eluent.

*4.1.1.1. 3-(2,3,5,6-tetrafluoro-4-(trifluoromethyl)phenoxy)-9H-xanthen-9-one (**6**).* Starting from 3-hydroxy-9*H*-xanthen-9-one (0.42 g, 2.0 mmol), octafluorotoluene (0.28 mL, 2.0 mmol), TBAHS (0.34 g, 1.0 mmol) and following the previously described general procedure a crude was obtained. FCC purification using PE/EA 9:1 as eluent afforded **6** as white solid, 0.74 g, yield 85%, mp 88–90 °C. ^{1}H NMR δ 7.01 (d, J = 2.0 Hz, 1H, H-4), 7.07 (dd, J = 2.4 and 8.4 Hz, 1H, H-2), 7.40 (t, J = 8.0 Hz, 1H, Ar), 7.44 (d, J = 8.0 Hz, 1H, H-5), 7.74 (t, J = 8.0 Hz, 1H, Ar), 8.33 (d, J = 8.0 Hz, 1H, Ar), 8.38 (d, J = 8.0 Hz, 1H, Ar). ^{19}F NMR δ −151.0 (m, 2F), −139.1 (m, 2F), −55.9 (t, J = 21.8 Hz, 3F).

4.1.1.2. (E,Z)(1-(4-(2,3,5,6-tetrafluoro-4-(trifluoromethyl)phenoxy) phenyl)but-1-ene-1,2-diyl)dibenzene (16 i.m.). Starting from **13 i.m.** (0.60 g, 1.2 mmol), octafluorotoluene (0.17 mL, 1.2 mmol), TBAHS (0.20 g, 0.60 mmol) and following the previously described general procedure a crude was obtained. FCC purification using PE/EA 9.85: 0.15 as eluent allowed separation of the isomers **16** and **16a**.

*(Z)-(1-(4-(2,3,5,6-tetrafluoro-4-(trifluoromethyl)phenoxy)phenyl)but-1-ene-1,2-diyl)dibenzene **16**.* Rf = 0.22, white solid, 0.6 g, yield 38%, mp 142–144 °C. ^{1}H NMR δ 0.97 (t, J = 7.2 Hz, 3H, CH_3), 2.51 (q, J = 7.2 Hz, 2H, CH_2), 6.49 (d, J = 8.0 Hz, 2H, H-3 and H-5), 6.75 (d, J = 8.0 Hz, 2H, H-2 and H-6), 7.10–7.22 (m, 4H, Ar), 7.25–7.31 (m, 4H, Ar), 7.35 (d, J = 8.0 Hz, 2H, Ar). ^{19}F NMR δ −152.0 (m, 2F), −139.4 (m, 2F), −55.5 (t, J = 21.8 Hz, 3F).

*(E)-(1-(4-(2,3,5,6-tetrafluoro-4-(trifluoromethyl)phenoxy)phenyl)but-1-ene-1,2-diyl)dibenzene **16a**.* Rf = 0.16, white solid, 0.25 g, yield 15%, mp 126–128 °C. ^{1}H NMR δ 0.97 (t, J = 7.2 Hz, 3H, CH_3), 2.47 (q, J = 7.2 Hz, 2H, CH_2), 6.78–6.82 (m, 4H, Ar), 6.98–7.28 (m, 4H, Ar), 7.25–7.31 (m, 4H, Ar), 7.38 (d, J = 8.0 Hz, 2H, Ar).

4.1.1.3. 1,2,4,5-tetrafluoro-3-(4-(1-(4-methoxyphenyl)-2-phenylbut-1-en-1-yl)phenoxy)-6-(trifluoromethyl)benzene (17 i.m.). Starting from **15 i.m.** (0.50 g, 1.5 mmol), octafluorotoluene (0.22 mL, 1.5 mmol), TBAHS (0.21 g, 0.75 mmol) and following the previously described general procedure **17 i.m.** was obtained that was then subjected to FCC (PE/DCM 9:1) to afford pure **17** and **17a**.

*(Z)-1,2,4,5-tetrafluoro-3-(4-(1-(4-methoxyphenyl)-2-phenylbut-1-en-1-yl)phenoxy)-6-(trifluoromethyl)benzene **17**.* Rf = 0.27, white solid, 0.52 g, yield 45%, mp 78–80 °C. ^{1}H NMR δ 0.98 (t, J = 7.2 Hz, 3H, CH_3), 2.52 (q, J = 7.2 Hz, 2H, CH_2), 3.84 (s, 3H, OCH_3), 6.64 (d, J = 8.0 Hz, 2H, H-3 and H-5), 6.85 (d, J = 8.0 Hz, 2H, H-2 and H-6), 7.03 (d, J = 8.8 Hz, 2H, H-3′ and H-5′), 7.10 (d, J = 8.8 Hz, 2H, H-2′ and H-6′), 7.16–7.34 (m, 5H, Ar). ^{19}F NMR δ −152.0 (m, 2F), −140.6 (m, 2F), −55.8 (t, J = 21.8 Hz, 3F).

*(E)-1,2,4,5-tetrafluoro-3-(4-(1-(4-methoxyphenyl)-2-phenylbut-1-en-1-yl)phenoxy)-6-(trifluoromethyl)benzene **17a**.* Rf = 0.22, white solid, 0.35 g, yield 22%, mp 55–58 °C. ^{1}H NMR δ 0.91 (t, J = 7.6 Hz, 3H, CH_3), 2.45 (q, J = 7.2 Hz, 2H, CH_2), 3.68 (s, 3H, OCH_3), 6.54 (dd, J = 1.6 and 8.4 Hz, 2H, Ar), 6.75 (dd, J = 2.0 and 8.4 Hz, 2H, Ar), 6.96 (d, J = 8.4 Hz, 2H, Ar), 7.09–719. (m, 5H, Ar), 7.21 (d, J = 8.4 Hz, 2H, Ar).

4.1.2. McMurry reaction. General procedure for the synthesis of TPE-based compounds (7 i.m, 13–15 i.m)

$TiCl_4$ (3.0 eq) was added to a stirred suspension of Zn powder (6.0 eq) in dry THF (1.5 mL/mmol), under N_2 atmosphere, at −15 °C. The mixture was heated under reflux for 1 h. The suspension was again cooled to −5 °C and the selected carbonyl compounds (1 eq) dissolved in THF (5 mL/mmol) were slowly added, and the mixture was refluxed for 2 h. After cooling, the reaction mixture was poured into 10% aqueous K_2CO_3 and extracted with Et_2O. The organic phase was washed with brine, dried over Na_2SO_4, and the solvent was removed under reduced pressure. The crude material was purified by FCC or fractionated crystallization from suitable solvent.

4.1.2.1. (E,Z)-9-(1-phenylpropylidene)-9H-xanthen-3-ol (7 i.m.). $TiCl_4$ (0.85 g, 4.5 mmol), Zn (0.60 g, 9.0 mmol), **6** (0.64 g, 1.5 mmol), and propiophenone (0.20 g, 1.5 mmol) were reacted according to the McMurray general procedure. The crude of reaction was purified by FCC (*n*-hexane/EtOAc 9.95:0.05) to obtain **7** and **7a**.

*(Z)-9-(1-phenylpropylidene)-3-(2,3,5,6-tetrafluoro-4-(trifluoromethyl) phenoxy)-9H-xanthene **7**.* Rf = 0.18, transparent oil, 0.27 g, 34% yield. ^{1}H NMR δ 0.97 (t, J = 7.6 Hz, 3H, CH_3), 2.81 (q, J = 7.6 Hz, 2H, CH_2), 6.26 (dd, J = 2.8 and 9.2 Hz, 1H, H-2), 6.49 (d, J = 9.2 Hz, 1H, H-1), 6.71 (d, J = 2.8 Hz, 1H, H-4), 7.08 (d, J = 6.8 Hz, 2H, Ar), 7.17–7.31 (m, 6H, Ar), 7.58 (d, J = 7.6 Hz, 1H, Ar).

*(E)-9-(1-phenylpropylidene)-3-(2,3,5,6-tetrafluoro-4-(trifluoromethyl) phenoxy)-9H-xanthene **7a**.* Rf = 0.21, transparent oil, 0.21 g, 26% yield. ^{1}H NMR δ 0.97 (t, J = 7.6 Hz, 3H, CH_3), 2.77 (q, J = 7.6 Hz, 2H, CH_2), 6.52 (dd, J = 2.8 and 8.4 Hz, 1H, H-2), 6.60–6.64 (m, 1H, Ar), 6.84–6.86 (m, 2H, Ar), 7.03–7.09 (m, 4H, Ar), 7.24–7.31 (m, 3H, Ar), 7.55 (dd, J = 1.6 and 7.6 Hz, 1H, Ar).

4.1.2.2. (E,Z)-4-(1,2-diphenylbut-1-en-1-yl)phenol (13 i.m.). $TiCl_4$ (1.14 g, 6.0 mmol), Zn (0.8 g, 12.0 mmol), 4-hydroxyphenylphenylmethanone **10** (0.39 g, 2.0 mmol), and propiophenone (0.33 g, 2.0 mmol) were reacted according to the McMurray general procedure. The crude of reaction was purified by FCC (PE/EA 8:2) to obtain **13 i.m.** as 2:1 mixture of *Z/E* isomers (0.59 g, 95% yield). ^{1}H NMR δ 0.9–1.03 (m, 3H, CH_3), 2.45–2.60 (m, 2H, CH_2), 4.55 (s, 0.66H, OH), 4.79 (s, 0.33H, OH), 6.50 (d, J = 8.4 Hz, 1.33H, Ar), 6.72 (d, J = 8.4 Hz, 1.33H, Ar), 6.82 (d, J = 8.8 Hz, 0.66H, Ar), 6.91 (d, J = 8.8 Hz, 0.66H, Ar), 7.00–7.45 (m, 10*H*, Ar).

4.1.2.3. (E,Z)-4-(1,2-bis-4-fluorophenylbut-1-en-1-yl)phenol (14 i.m. and 14). $TiCl_4$ (2.28 g, 12.0 mmol), Zn (1.6 g, 24.0 mmol), 4-fluorophenyl-4-hydroxyphenylmethanone **11** (0.83 g, 4.0 mmol), and 4-fluoropropiophenone (0.94 g, 4.0 mmol) were reacted according to the McMurray general procedure. The crude of reaction was purified by fractioned crystallization from isopropyl alcohol to afford the desired *trans* isomer (*E*)-4-(1,2-bis-4-fluorophenylbut-1-en-1-yl)phenol **14** (0.66 g, 83% yield), mp 95–96 °C. ^{1}HNMR δ 0.94 (t, J = 7.2 Hz, 3H, CH_3), 2.44 (q, J = 7.2 Hz, 2H, CH_2), 3.8 (br, 1H, OH), 6.56 (d, J = 8.8 Hz, 2H, Ar), 6.75 (d, J = 8.4 Hz, 2H, Ar), 6.82–6.94 (m, 2H, Ar), 7.01–7.08 (m, 4H, Ar), 7.10–7.14 (m, 2H, Ar).

4.1.2.4. (E,Z)-4-(1-(4-methoxyphenyl)-2-phenylbut-1-en-1-yl)phenol (15

i.m.). $TiCl_4$ (1.14 g, 6.0 mmol), Zn (0.8 g, 12.0 mmol), 4-hydroxyphenyl-4-methoxyphenylmethanone **12** (0.46 g, 2.0 mmol), and propiophenone (0.33 g, 2.0 mmol) were reacted according to the McMurray general procedure. The crude of reaction was purified by FCC (PE/EA 7:3) to obtain **15 i.m.** as 1.5:1 mixture of *cis/trans* isomers (0.5 g, 75% yield). ^{1}H NMR δ 2.52 (t, J = 7.2 Hz, 3H, CH_3), 2.54 (q, J = 7.2 Hz, 2H, CH_2), 3.68 (s, 1.2H, OCH_3), 3.89 (s, 1.8H, OCH_3), 6.42 (d, J = 8.8 Hz, 1.2H, Ar), 6.48 (d, J = 8.8 Hz, 0.8H, Ar), 6.78 (d, J = 8.8 Hz, 1.2H, Ar), 6.80–6.83 (m, 0.8H, Ar), 6.89 (d, J = 8.8 Hz, 1.2H, Ar), 7.02–7.43 (m, 7.8H, Ar).

*4.1.3. Removal of the perfluorotolyl function. General procedure for the synthesis of **8, 13, 13a, 15***

The perfluorotolyl ether (**7**, **16**, **16a**, **17**, 1.0 eq) dissolved in dry DMF (100 mL/mmol) was treated with freshly prepared NaOMe (100 eq) and the reaction mixture was stirred in the dark for 1.5 h. The solution was diluted with water (100 mL/mmol), acidified with 10% aq HCl, and extracted with EtOAc. The combined organic extracts were washed with brine, dried and over Na_2SO_4, and the solvent was evaporated *in vacuo*.

*4.1.3.1. (Z)-9-(1-phenylpropylidene)-9H-xanthen-3-ol **(8)***. Starting from **7** (0.27 g, 0.63 mmol), NaOMe (3.34 g, 63 mmol) a crude was obtained that was crystallized from isopropyl alcohol to obtain **8** (0.11 g, 88% yield), as colourless crystals, mp 60–62 °C. ^{1}H NMR δ 0.97 (t, J = 7.5 Hz, 3H, CH_3), 2.79 (q, J = 7.5 Hz, 2H, CH_2), 6.17 (dd, J = 8.7 and 2.5 Hz, 1H, H-2), 6.47 (d, J = 8.7 Hz, 1H, H-1), 6.66 (d, J = 2.5 Hz, 1H, H-4), 7.08 (dd, J = 7.8 and 1.8 Hz, 1H, H-5), 7.11–7.26 (m, 7H, Ar), 7.62 (dd, J = 7.8 and 1.8 Hz, 1H, H-8).

*4.1.3.2. (Z)-4-(1,2-diphenylbut-1-en-1-yl)phenol **(13)***. Starting from **16** (0.6 g, 1.1 mmol), NaOMe (5.9 g, 110.0 mmol) a crude was obtained that was crystallized from isopropyl alcohol to give **13** (0.28 g, 77% yield) as colourless crystals, mp 129–131 °C. ^{1}H NMR δ 0.94 (t, J = 7.4 Hz, 3H, CH_3), 2.48 (q, J = 7.4 Hz, 2H, CH_2), 4.53 (br, 1H, OH), 6.51 (d, J = 8.8, 2H, H-3 and H-5), 6.75 (d, J = 8.8 Hz, 2H, H-2 and H-6), 7.08–7.19 (m, 5H, Ar), 7.21–7.29 (m, 3H, Ar), 7.31–7.36 (m, 2H, Ar). Analytical data of this intermediate are in good agreement with the literature data [44].

*4.1.3.3. (Z)-4-(1,2-diphenylbut-1-en-1-yl)phenol **(13a)***. Starting from **16a** (0.27 g, 0.63 mmol), NaOMe (3.34 g, 63.0 mmol) a crude was obtained that was crystallized from methyl alcohol to give **13a** colourless crystals (0.19 g, 31% yield), mp 106–108 °C. ^{1}H NMR δ 0.94 (t, J = 7.4 Hz, 3H, CH_3), 2.48 (q, J = 7.4 Hz, 2H, CH_2), 4.84 (br, 1H, OH), 6.75 (d, J = 8.4 Hz, 2H, H-3 and H-5), 6.85 (d, J = 8.4 Hz, 2H, H-2 and H-6), 7.05 (d, J = 8.4 Hz, 2H, Ar), 7.10–7.20 (m, 8H, Ar). Analytical data of this intermediate are in good agreement with the literature data [44].

*4.1.3.4. (E)-4-(1-(4-methoxyphenyl)-2-phenylbut-1-en-1-yl)phenol **(15)***. Starting from **17** (0.52 g, 1.57 mmol) and NaOMe (8.4 g, 157.0 mmol) a crude was obtained that purified by FCC (EP/EA 7:3) to obtain **15**, 0.50 g, 96% yield, mp 113–116 °C. ^{1}H NMR δ 0.96 (t, J = 7.4 Hz, 3H, CH_3), 2.51 (q, J = 7.4 Hz, 2H, CH_2), 3.83 (s, 3H, OCH_3), 4.75 (br, 1H, OH), 6.49 (d, J = 8.2 Hz, 2H, Ar), 6.64 (d, J = 8.4 Hz, 2H, Ar), 6.85 (d, J = 8.4 Hz, 2H, Ar), 7.09–7.19 (m, 7H, Ar).

*4.1.4. Williamson reaction: General procedure (compounds **9, 18–20**)*.

To a solution of phenol derivative (**8**, **13**, **13a**, **14**, **15**, 1.0 eq) in acetone (20 mL/mmol) was added K_2CO_3 (1.3 eq), followed by alkyl bromide (1.3 eq). The reaction mixture was heated at reflux for 4–8 h at 80 °C (monitored by TLC). Upon reaction completion, the mixture was filtered, and the solvent evaporated under reduced pressure. The resulting crude product was purified by column by FCC (PE/EA 9:1) to give the desired products.

*4.1.4.1. (Z)-3-(2-bromoethoxy)-9-(1-phenylpropylidene)-9H-xanthene **(9)***. Starting from **8** (0.19 g, 0.6 mmol), 1,2-dibromoethane (0.09 g, 0.78 mmol), K_2CO_3 (0.1 g, 0.78 mmol) and following the general Williamson procedure, **9** was obtained as oily product, (0.36 g, 85% yield). ^{1}H NMR δ 0.97 (t, J = 7.5 Hz, 3H, CH_3), 2.78 (q, J = 7.5 Hz, 2H, CH_2), 3.58 (t, J = 6.5 Hz, 2H, CH_2Br), 4.20 (t, J = 6.5 Hz, 2H, OCH_2), 6.19 (dd, J = 8.7 and 2.5 Hz, 1H, H-2), 6.42 (d, J = 8.7 Hz, 1H, H-1), 6.65 (d, J = 2.5 Hz, 1H, H-4), 7.09 (dd, J = 7.8 and 1.8 Hz, 1H, H-5), 7.12–7.29 (m, 7H, Ar), 7.58 (dd, J = 7.8 and 1.8 Hz, 1H, H-8).

*4.1.4.2. (Z)-(1-(4-(prop-2-yn-1-yloxy)phenyl)but-1-ene-1,2-diyl) dibenzene **(18)***. Starting from **13** (0.28 g, 0.93 mmol), 3-bromoprop-1-yne (0.14. g, 1.2 mmol), K_2CO_3 (0.17 g, 1.2 mmol) and following the general Williamson procedure, **18** was obtained as oily product, (0.29 g, 98% yield). ^{1}H NMR δ 0.94 (t, J = 7.4 Hz, 3H, CH_3), 2.48–2.52 (m, 3H, CH_2 and CH), 4.57 (d, J = 2.4 Hz, 2H, OCH_2), 6.63 (d, J = 8.9 Hz, 2H, H-3 and H-5), 6.81 (d, J = 8.9 Hz, 2H, H-2 and H-6), 7.12–7.24 (m, 4H, Ar), 7.27–7.35 (m, 4H, Ar), 7.23–7.29 (m, 2H, Ar).

*4.1.4.3. (E)-(1-(4-(prop-2-yn-1-yloxy)phenyl)but-1-ene-1,2-diyl) dibenzene **(18a)***. Starting from **13a** (0.19 g, 0.6 mmol), 3-bromoprop-1-yne (0.18 g, 0.9 mmol), K_2CO_3 (0.11 g, 0.9 mmol) and following the general Williamson procedure, **18a** was obtained as oily product, (0.12 g, 98% yield). ^{1}HNMR δ 0.95 (t, J = 7.4 Hz, 3H, CH_3), 2.47 (m, 3H, CH_2 and CH), 4.76 (d, J = 2.4 Hz, 2H, OCH_2), 6.85 (d, J = 8.8 Hz, 2H, Ar), 6.90 (d, J = 8.9 Hz, 2H, Ar), 6.99–7.01 (m, 4H, Ar), 7.06–7.14 (m, 4H, Ar), 7.19 (d, J = 8.8 Hz, 2H, Ar).

*4.1.4.4. (E)-4,4′-(1-(4-(prop-2-yn-1-yloxy)phenyl)but-1-ene-1,2-diyl)bis (fluorobenzene) **(19)***. Starting from **14** (0.33 g, 0.98 mmol), 3-bromoprop-1-yne (0.15. g, 1.3 mmol), K_2CO_3 (0.18 g, 1.3 mmol) and following the general Williamson procedure, **19** was obtained as oily product, (0.35 g, 95% yield). ^{1}H NMR δ 0.92 (t, J = 7.2 Hz, 3H, CH_3), 2.44–2.49 (m, 3H, CH_2 and CH), 4.58 (d, J = 2.9 Hz, 2H, OCH_2), 6.58 (d, J = 8.8 Hz, 2H, Ar), 6.73 (d, J = 8.4 Hz, 2H, Ar), 6.82–6.91 (m, 2H, Ar), 7.03–7.07 (m, 4H, Ar), 7.09–7.13 (m, 2H, Ar).

*4.1.4.5. (Z)-1-methoxy-4-(2-phenyl-1-(4-(prop-2-yn-1-yloxy)phenyl)but-1-en-1-yl)benzene **(20)***. Starting from **15** (0.52 g, 1.57 mmol), 3-bromoprop-1-yne (0.24. g, 2.0 mmol), K_2CO_3 (0.27 g, 2.0 mmol) and following the general Williamson procedure, **20** was obtained as oily product, (0.53 g, 94% yield). ^{1}H NMR δ 0.94 (t, J = 7.4 Hz, 3H, CH_3), 2.46–2.50 (m, 3H, CH_2 and CH), 3.83 (s, 3H, OCH_3), 4.57 (d, J = 2.4 Hz, 2H, OCH_2), 6.59 (d, J = 8.9 Hz, 2H, Ar), 6.79 (d, J = 8.9 Hz, 2H, Ar), 6.85 (d, J = 8.9 Hz, 2H, Ar), 7.21–7.19 (m, 7H, Ar).

*4.1.5. (Z)-1-(2-((9-(1-phenylpropylidene)-9H-xanthen-3-yl)oxy)ethyl) pyrrolidine hydrochloride **(1)***.

Compound **9** (0.3 g, 0.71 mmol) was dissolved in THF (15 mL), then pyrrolidine (0.075 g, 1.06 mmol) and Et_3N (0.1 g, 1.06 mmol) were added and the solution was stirred at r.t. in the dark for 18 h. The reaction mixture was poured into 3 M HCl (25 mL) and extracted with DCM (3 × 30 mL); the combined organic extracts were washed with 0.5 M NaOH (3 × 30 mL), brine (1 × 30 mL), dried over Na_2SO_4, filtered and concentrated to dryness. The crude of reaction was purified by FCC using DCM/MeOH 95:5 as eluent to obtain **1** (0.26 g, 90% yield) mp 104–106 °C. ^{1}H NMR δ 0.97 (t, J = 7.5 Hz, 3H, CH_3), 1.83–1.89 (m, 4H, CH_2-pyrrolidine), 2.75–2.80 (m, 6H, CH_2N-pyrrolidine, CH_2), 2.96 (t, J = 6.0 Hz, 2H, CH_2N), 4.08 (t, J = 6.5 Hz, 2H, CH_2O), 6.19 (dd, J = 8.0 and 1.2 Hz, 1H, H-2), 6.40 (d, J = 8.8 Hz, 1H, H-1), 6.64 (dd, J = 8.4, and 2.4 Hz, 1H, H-4), 7.09 (dd, J = 7.8 and 1.8 Hz, 1H, H-5), 7.14–7.29 (m, 7H, Ar), 7.57 (dd, J = 7.8 and 1.8 Hz, 1H, H-8). ^{13}C NMR δ 13.4 (CH_3), 23.6 (2C, CH_2-pyrrolidine), 28.5 (CH_2), 54.8 (2C, CH_2N-pyrrolidine), 55.1 (CH_2N), 67.4 (CH_2O), 102.3, 110.0, 116.0, 118.4, 122.2, 123.4, 126.2, 126.5, 127.0, 128.3 (2C), 128.8, 129.0, 129.6

(2C), 139.2, 142.7, 153.8, 155.6, 158.9. ESI-MS (*m/z*): 413 (M + H).

*4.1.6. Mannich reaction: General procedure (compounds **2, 2a, 3, 5, 21**)*

To a suspension of formaldehyde (1.5 eq), the selected amine (1.5 eq), and $CuSO_4$ (16 mg/mmol), a H_2O/EtOH 1:1 solution (10 mL/mmol) of propargyl derivative (1.0 eq) was added. The mixture was heated at reflux for 24 h. After cooling, NH_4OH solution (15 mL/mmol) was added and the mixture was extracted with Et_2O, the combined organic layers were dried over Na_2SO_4 and the solvent was evaporated *in vacuo* to obtain an oily crude which was purified by FCC.

*4.1.6.1. ((Z)-1-(4-(4-(1,2-diphenylbut-1-en-1-yl)phenoxy)but-2-yn-1-yl) pyrrolidine (**2**).* Starting from **18** (0.2 g, 0.53 mmol), formaldehyde (0.002 g, 0.8 mmol), $CuSO_4$ (9 mg), and pyrrolidine (0.06 g, 0.8 mmol) following the above described general procedure, **2** was obtained as a white oil. FCC purification PE/EA 1:1, (0.17 g, 75% yield), mp 132–135 °C. ^{1}H NMR δ 0.93 (t, J = 7.6 Hz, 3H, CH_3), 1.76–1.79 (m, 4H, CH_2-pyrrolidine), 2.46 (q, J = 7.5 Hz, 2H, CH_2), 2.47–2.54 (m, 4H, CH_2N-pyrrolidine), 3.41 (s, 2H, CH_2N), 4.58 (s, 2H, OCH_2), 6.60 (d, J = 8.8 Hz, 2H, H-3 and H-5), 6.78 (d, J = 8.8 Hz, 2H, H-2 and H-6), 7.12–7.14 (m, 3H, Ar), 7.16–7.20 (m, 2H, Ar), 7.23–7.29 (m, 3H, Ar), 7.34–7.37 (m, 2H, Ar). ^{13}C NMR δ 13.5 (CH_3), 24.2 (2C, CH_2-pyrrolidine), 28.8 (CH_2), 42.7 (CH_2N), 51.8 (2C, CH_2N-pyrrolidine), 55.2 (CH_2N), 75.1, 77.2, 85.8, 114.5 (2C), 125.8 (2C), 126.2, 127.4 (2C), 127.7(2C), 129.6 (2C), 130.5, 130.6(2C), 137.4, 137.9, 141.9, 142.4, 143.1. ESI-MS (*m/z*): 423 (M + H).

*4.1.6.2. (E)-1-(4-(4-(1,2-diphenylbut-1-en-1-yl)phenoxy)but-2-yn-1-yl) pyrrolidine (**2a**).* Starting from **18a.** (0.1 g, 0.26 mmol), formaldehyde (0.001 g, 0.4 mmol), $CuSO_4$ (4.5 mg), and pyrrolidine (0.03 g, 0.4 mmol) following the above described general procedure, **2a** was obtained as a white oil. FCC purification PE/EA 1:1, 0.09 g, 75% yield, hydrochloride salt mp 127–129 °C. ^{1}H NMR δ 0.91 (t, J = 7.6 Hz, 3H, CH_3), 1.79–2.08 (m, 4H, CH_2-pyrrolidine), 2.45 (q, J = 7.5 Hz, 2H, CH_2), 2.96–3.08 (m, 2H, CH_2N-pyrrolidine), 2.55–2.63 (m, 2H, CH_2N-pyrrolidine), 3.96 (s, 2H, OCH_2), 4.76 (s, 2H, CH_2N), 6.60 (d, J = 8.8 Hz, 2H, H-3 and H-5), 6.78 (d, J = 8.8 Hz, 2H, H-2 and H-6), 7.12 (d, J = 7.6 Hz, 4H, Ar), 7.16 (d, J = 7.6 Hz, 1H, Ar), 7.23–7.29 (m, 4H, Ar), 7.34 (d, J = 7.8 Hz, 1H, Ar). ^{13}C NMR δ 13.6 (CH_3), 24.1 (2C, CH_2-pyrrolidine), 28.7 (CH_2), 42.7 (CH_2N), 51.8 (2C, CH_2N-pyrrolidine), 55.2 (CH_2N), 75.1, 77.2, 85.8, 113.8 (2C), 126.2, 126.7 (2C), 128.0 (2C), 128.2 (2C), 129.6 (2C), 129.8 (2C), 132.0, 136.5, 138.2, 141.8, 142.5, 143.8. ESI-MS (*m/z*): 423 (M + H).

*4.1.6.3. (Z)-1-(4-(4-(1,2-diphenylbut-1-en-1-yl)phenoxy)but-2-yn-1-yl) piperidine hydrochloride (**3**).* Starting from **18** (0.2 g, 0.53 mmol), formaldehyde (0.002 g, 0.8 mmol), $CuSO_4$ (9 mg), piperidine (0.06 g, 0.8 mmol), and following the above described general procedure, **3** was obtained as a white oil. FCC purification: PE/EA 1:1, (0.2 g, 90% yield). ^{1}H NMR δ 0.93 (t, J = 7.6 Hz, 3H, CH_3), 1.60–1.80 (m, 6H, CH_2-piperidine), 2.45 (q, J = 7.5 Hz, 2H, CH_2), 2.46–2.52 (m, 4H, CH_2N-piperidine), 3.34 (s, 2H, CH_2N), 4.59 (s, 2H, OCH_2), 6.61 (d, J = 8.8 Hz, 2H, H-3 and H-5), 6.79 (d, J = 8.8 Hz, 2H, H-2 and H-6), 7.12 (d, J = 7.6 Hz, 4H, Ar), 7.16 (d, J = 7.6 Hz, 1H, Ar), 7.23–7.29 (m, 4H, Ar), 7.34 (d, J = 7.8 Hz, 1H, Ar). ^{13}C NMR δ 13.7 (CH_3), 24.1, 25.1 (2C, CH_2-piperidine), 29.2 (CH_2), 43.2 (CH_2N), 53.9 (2C, CH_2N-piperidine), 55.8, 77.9, 87.4, 113.8 (2C), 126.2, 126.7 (2C), 128.0 (2C), 128.3 (2C), 129.6 (2C), 129.8 (2C), 132.0, 136.5, 138.2, 141.8, 142.5, 143.8, 155.7. ESI-MS (*m/z*): 437 (M + H).

*4.1.6.4. (E)-4-(4-(1,2-bis(4-fluorophenyl)but-1-en-1-yl)phenoxy)-N,N-diethylbut-2-yn-1-amine (**5**).* Starting from **19** (0.2 g, 0.53 mmol), formaldehyde (0.002 g, 0.8 mmol), $CuSO_4$ (9 mg), diethylamine (0.06 g, 0.8 mmol), and following the above described general procedure **5** was obtained as a white oil. FCC purification PE/EA 1:1, (0.18 g, 78% yield). ^{1}H NMR δ 0.94 (t, J = 7.2 Hz, 3H, CH_3), 1.65 (t, J = 5.7 Hz, 6H, CH_3), 2.40 (q, J = 7.2 Hz, 2H, CH_2), 2.41–2.48 (m, 4H, CH_2N), 3.26 (s, 2H, NCH_2), 4.52 (s, 2H, OCH_2), 6.56 (d, J = 8.8 Hz, 2H, H-3 and H-5), 6.77 (d, J = 8.4 Hz, 2H, H-2 and H-6), 6.84–6.96 (m, 2H, Ar), 7.00–7.05 (m, 4H, Ar), 7.11–7.15 (m, 2H, Ar). ^{13}C NMR δ 9.8 (2C, CH_3), 13.6 (CH_3), 29.1 (CH_2), 41.6 (NCH_2), 47.9 (2C, CH_2N), 55.8, 77.4, 86.5, 113.8 (2C), 115.0 (d, J = 20.6 Hz, 2C), 115.2 (d, J = 21.4 Hz, 2C), 131.1 (d, J = 8.3 Hz, 2C), 131.2 (d, J = 7.6 Hz, 2C), 132.1 (2C), 136.0, 137.6, 138.1 (d, J = 3.8 Hz,), 139.5 (d, J = 3.1 Hz,), 141.0, 156.4, 161.4 (d, J = 246.2 Hz), 161.8 (d, J = 246.2 Hz). ESI-MS (*m/z*): 461 (M + H).

*4.1.6.5. ((Z)-1-(4-(4-(1-(4-methoxyphenyl)-2-phenylbut-1-en-1-yl) phenoxy)but-2-yn-1-yl)piperidine (**21**).* Starting from **20** (0.53 g, 1.44 mmol), formaldehyde (0.005 g, 2.17 mmol), $CuSO_4$ (24 mg), piperidine (0.16 g, 2.17 mmol), and following the above described general procedure, **21** was obtained as a yellowish oil. FCC purification DCM/MeOH 95:0.5, (0.37 g, 55% yield). ^{1}H NMR δ 0.93 (t, J = 7.4 Hz, 3H, CH_3), 1.61–1.80 (m, 6H, CH_2-piperidine), 2.46 (q, J = 7.4 Hz, 2H, CH_2), 2.49–2.53 (m, 4H, CH_2 piperidine), 3.25 (s, 2H, NCH_2), 3.86 (s, 3H, OCH_3), 4.58 (s, 2H, OCH_2), 6.60 (d, J = 8.9 Hz, 2H, Ar), 6.80 (d, J = 8.9 Hz, 2H, Ar), 6.87 (d, J = 8.9 Hz, 2H, Ar), 7.09 (d, J = 8.9 Hz, 2H, Ar), 7.12–7.16 (m, 5H, Ar).

*4.1.7. (Z)-4-(2-phenyl-1-(4-((4-(piperidin-1-yl)but-2-yn-1-yl)oxy)phenyl) but-1-en-1-yl)phenol (**4**)*

A 1.0 M solution of BBr_3 in DCM (1.2 mL, 1.2 mmol) was slowly added to a solution of **21** (0.37 g, 0.8 mmol) in dry DCM maintained at −78 °C, under nitrogen atmosphere. The reaction mixture was stirred at the same temperature for 1 h and then at r.t. for 4 h. The reaction was cooled at 0 °C and then quenched by adding MeOH. The solvent was removed under reduced pressure and the crude product was purified by FCC using mixture of DCM/MeOH 95:05 as eluent to obtain **4** as brown oil (0.24 g, 67% yield). ^{1}H NMR (Acetone-d_6) δ 0.95 (t, J = 7.4 Hz, 3H, CH_3), 1.58–1.79 (m, 6H, CH_2-piperidine) 2.49 (q, J = 7.4 Hz, 2H, CH_2), 2.46–2.56 (m, 4H, CH_2N-piperidine), 3.28 (s, 2H, NCH_2), 4.59 (s, 2H, OCH_2), 6.75 (d, J = 8.9 Hz, 2H, Ar), 6.83 (d, J = 8.9 Hz, 2H, Ar), 6.88 (d, J = 8.9 Hz, 2H, Ar), 7.12 (d, J = 8.9 Hz, 2H, Ar), 7.13–7.20 (m, 5H, Ar). ^{13}C NMR (Acetone-d_6) δ 13.7 (CH_3), 24.1, 25.1 (2C, CH_2-piperidine), 29.2 (CH_2), 43.2 (NCH_2), 53.9 (2C, CH_2N-piperidine), 55.8, 77.9, 87.4, 113.8 (2C), 114.1 (2C), 126.6 (2C), 128.0 (2C), 128.4 (2C), 129.7 (2C), 132.0, 136.5, 138.2, 141.8, 142.5, 143.8, 155.5, 155.7. ESI-MS (*m/z*): 453 (M + H).

4.2. Cell cultures

The MCF-7 (ER +) and MDA-MB-231 (ER −) human breast cancer cells were obtained from LGC standard (Teddington, Middlesex, UK). Human Jurkat T leukemia cells were purchased from Istituto Zooprofilattico of Brescia (Italy). Human breast cancer cell lines MCF-7 and MDA-MB-231 were grown in adhesion and propagated in Eagle's Minimum Essential Medium (EMEM) (ATCC Manassas, VA, USA) or Dulbecco's Modified Eagle's Medium (DMEM) (ATCC), respectively, both supplemented with 10% heat-inactivated fetal bovine serum (FBS) (Biochrome, a division of Harvard Bioscience, Inc, Holliston, MA, USA) and 1% penicillin/streptomycin solution 100 U/mL (Sigma-Aldrich, Saint Louis, MO, USA). Twenty-four hours before and during treatments, cells were estrogen-depleted by culturing them in complete medium where FBS was substituted with Dextran-Coated Charcoal (DCC) – FBS (Sigma-Aldrich). DCC-FBS was prepared following manufacturer's protocol. Jurkat cell line was grown in suspension and propagated in RPMI 1640 (ATCC), supplemented with 10% heat-inactivated FBS, 1% L-glutamine and 1% penicillin/streptomycin solution. All cell lines were maintained at 37 °C in a humidified atmosphere containing 5% CO_2.

4.3. Cell treatments

Since TAM's activity can be markedly influenced by the level of estrogens in culture, in order to lower any possible interference in the study due to the presence of estrogens in serum, all experiments were conducted in serum depleted by steroids [45]. 20 000 MCF-7 or MDA-MB-231/200 μL of complete medium per well were seeded in a 96 wells plate. After incubation over-night, complete medium was substituted with DCC-FBS complete medium, in order to deplete estrogens. After 24 h, cells were treated with increasing concentrations of TAM and compounds **1**–**5** (0–40 μM) in DCC-FBS complete medium. 24 h later, we proceeded to the analysis reported below.

In order to compare genotoxic potential of **1** with that of TAM, 1.5×10^6 of Jurkat cells were seeded in a 24-wells plate and treated with increasing concentrations of TAM or its derivative (0–20 μM) and then analyzed after 6 h.

4.4. Cell viability

To assess MCF-7 and MDA-MB-231 viability, an MTT test was performed. In brief, after treatments, medium was removed from each well, cells were incubated with a 10 μM MTT solution for 2 h at 37 °C, 5% CO_2, and washed. The formazan salts formed were dissolved in 150 μL of DMSO. The absorbance was measured at 570 nm using the TECAN microplate reader.

4.5. Analysis of p53, PARP, Bax, and Bcl-2 protein expression

After 24 h treatments, cells were harvested, fixed with 4% formaldehyde solution, permeabilized with 90% methanol solution and treated with the appropriated primary antibody: FITC-anti-PARP (1:20, Invitrogen, Carlsbad, CA, USA), antibody specific for the 85 kDa PARP cleaved portion; anti-p53 (1:500, Ancell corporation Bayport, MN, USA); anti Bcl-2 (1:100, Santa Cruz Biotechnology, Santa Cruz, CA, USA); anti-Bax (1:100, Santa Cruz Biotechnology, Santa Cruz, CA, USA). Non-labeled primary antibodies were incubated with a FITC-labeled secondary antibody (1:100, Sigma-Aldrich). EasyCyte 5HT (Merck Millipore, Darmstadt, Germany) was used to perform flow cytometric analyses. At least 5000 events were evaluated.

4.6. Analysis of p53, Bax, Bcl-2, and Bim mRNA expression

The RNA from MCF-7 cells was isolated using the mirVana miRNA Isolation Kit (Life Technologies, a division of ThermoFisher Scientific, Waltham, MA, USA), according to manufacturer's protocol. In brief, cells were lysed and the aqueous phase containing the nucleic acids was isolated through a liquid-liquid organic extraction in phenol-chloroform. To purify RNA, ethanol was added and the resulting solution was filtered through a filter cartridge containing a glass-fiber filter, which selectively immobilizes RNA. After washing with appropriate solutions, RNA was eluted with RNAase free water. NanoVue plus spectrophotometer (GE Healthcare UK) was used to perform RNA quantification. Total collected RNA was used for reverse transcription by High Capacity cDNA Reverse Transcription kit (Life Technologies). The absorbance was measured at 260 nm. 200 ng total RNA were added to 10 μL of the reaction kit mixture with RNase inhibitor according to manufacturer's instructions. The thermal cycler (cfx connect, Biorad Hercules, CA, USA) conditions were: 10 min at 25 °C, 120 min 37 °C, 5 min 85 °C and then 4 °C until their storage at −20 °C. Quantification of Bax, Bcl-2, p53, Bim and GADPH, as endogenous control, was performed in triplicate by real-time PCR (ABI Prism 7900HT, Life Technologies), using Universal Master Mix and TaqMan assays Hs00180269_m1 (Bax), Hs00608023_m1 (Bcl-2), Hs01034249_m1 (p53), Hs00708019_s1 (Bim) and Hs99999905_m1 (GADPH) (Life Technologies).

4.7. DNA damage

To assess the genotoxic potential of **1** and TAM, the phosphorylation of histone γ-H2A.X was measured, as a marker of double-strand DNA breaks. After 6 h treatment with TAM or **1**, cells were fixed, permeabilized and incubated for 30 min in the dark at room temperature with an anti-γ-H2A.X-Alexa Fluor488® antibody (5:100 Merck Millipore). Samples were analyzed via flow cytometry.

4.8. Statistical analysis

All results are expressed as the mean ± SEM of at least four different experiments. Differences in mRNA expression are reported as value ± SEM and represent the relative expression calculated through the 2-ΔΔCt method. One-way ANOVA, followed by Dunnett as post-test, was used to evaluate differences among treatments. GraphPad Prism for macOS version 6.00 (GraphPad Prism, GraphPad Software, La Jolla, California, USA) was used for all statistical analyses. $P < 0.05$ was considered significant.

Appendix A. Supplementary material

Supplementary data to this article can be found online at https://doi.org/10.1016/j.bioorg.2019.02.017.

References

[1] WHO. Available from: < https://www.who.int/cancer/PRGlobocanFinal.pdf > .
[2] https://seer.cancer.gov/csr/1975_2015/revisions.html. Updated: September 10, 2018.
[3] American Cancer Society, Breast Cancer Facts & Figures 2017–2018, American Cancer Society, Inc., Atlanta, 2017.
[4] C.M. Pfeffer, A.T.K. Singh, Apoptosis: a target for anticancer therapy, Int. J. Mol. Sci. 19 (2018).
[5] S. Haupt, M. Berger, Z. Goldberg, Y. Haupt, Apoptosis – the p53 network, J. Cell Sci. 116 (2003) 4077–4085.
[6] H. Rochefort, J.L. Borgna, E. Evans, Cellular and molecular mechanism of action of antiestrogens, J. Steroid Biochem. 19 (1983) 69–74.
[7] V.C. Jordan, Tamoxifen: a most unlikely pioneering medicine, Nat. Rev. Drug Discovery 2 (2003) 205–213.
[8] H. Brauch, V.C. Jordan, Targeting of tamoxifen to enhance antitumour action for the treatment and prevention of breast cancer: the 'personalised'approach? Eur. J. Cancer 45 (2009) 2274–2283.
[9] V.C. Jordan, Antiestrogens and selective estrogen receptor modulators as multifunctional medicines. 2. Clinical considerations and new agents, J. Med. Chem. 46 (2003) 1081–1111.
[10] H. Glatt, W. Davis, W. Meinl, H. Hermersdörfer, S. Venitt, D.H. Phillips, Rat, but not human, sulfotransferase activates a tamoxifen metabolite to produce DNA adducts and gene mutations in bacteria and mammalian cells in culture, Carcinogenesis 19 (1998) 1709–1713.
[11] G. Yang, S. Nowsheen, K. Aziz, A.G. Georgakilas, Toxicity and adverse effects of Tamoxifen and other anti-estrogen drugs, Pharmacol. Ther. 139 (2013) 392–404.
[12] M.-S. Chang, Tamoxifen resistance in breast cancer, Biomol. Ther. 20 (2012) 256–267.
[13] C. Rivera-Guevara, J. Camacho, Tamoxifen and its new derivatives in cancer research, Recent Pat. Anti-Cancer Drug Discov. 6 (2011) 237–245.
[14] S. Mandlekar, R. Yu, T.-H. Tan, A.-N.T. Kong, Activation of caspase-3 and c-Jun NH2-terminal kinase-1 signaling pathways in tamoxifen-induced apoptosis of human breast cancer cells, Cancer Res. 60 (2000) 5995–6000.
[15] G.J. Zhang, I. Kimijima, M. Onda, M. Kanno, H. Sato, T. Watanabe, A. Tsuchiya, R. Abe, S. Takenoshita, Tamoxifen-induced apoptosis in breast cancer cells relates to down-regulation of bcl-2, but not bax and bcl-X(L), without alteration of p53 protein levels, Clin. Cancer Res.: Off. J. Am. Assoc. Cancer Res. 5 (1999) 2971–2977.
[16] S. Ray, Sangita, The potent triaryiethylene pharmacophore, Drugs Future 29 (2004) 185–203.
[17] Shagufta, I. Ahmad, Tamoxifen a pioneering drug: an update on the therapeutic potential of tamoxifen derivatives, Eur. J. Med. Chem. 143 (2018) 515–531.
[18] A.F. Palermo, M. Diennet, M. El Ezzy, B.M. Williams, D. Cotnoir-White, S. Mader, J.L. Gleason, Incorporation of histone deacetylase inhibitory activity into the core of tamoxifen – a new hybrid design paradigm, Bioorg. Med. Chem. 26 (2018) 4428–4440.
[19] D. O'Hagan, R.J. Young, Accurate lipophilicity (log P) measurements inform on subtle stereoelectronic effects in fluorine chemistry, Angew. Chem. Int. Ed. 55 (2016) 3858–3860.
[20] E.F. Nuwaysir, Y.P. Dragan, R. McCague, P. Martin, J. Mann, V.C. Jordan, H.C. Pitot, Structure-activity relationships for triphenylethylene antiestrogens on

hepatic phase-I and phase-II enzyme expression, Biochem. Pharmacol. 56 (1998) 321–327.
[21] D.W. Robertson, J.A. Katzenellenbogen, D.J. Long, E.A. Rorke, B.S. Katzenellenbogen, Tamoxifen antiestrogens. A comparison of the activity, pharmacokinetics, and metabolic activation of the cis and trans isomers of tamoxifen, J. Steroid Biochem. 16 (1982) 1–13.
[22] A. Detsi, M. Koufaki, T. Calogeropoulou, Synthesis of (Z)-4-hydroxytamoxifen and (Z)-2-[4-[1-(p-hydroxyphenyl)-2-phenyl]-1butenyl]phenoxyacetic acid, J. Org. Chem. 67 (2002) 4608–4611.
[23] P.L. Coe, C.E. Scriven, Crossed coupling of functionalized ketones by low valent titanium (the Mcmurry reaction) – a new stereoselective synthesis of tamoxifen, J. Chem. Soc. Perk T 1 (1986) 475–477.
[24] A.B. Foster, M. Jarman, O.T. Leung, R. McCague, G. Leclercq, N. Devleeschouwer, Hydroxy derivatives of tamoxifen, J. Med. Chem. 28 (1985) 1491–1497.
[25] D.J. Collins, J.J. Hobbs, C.W. Emmens, Antiestrogenic and antifertility compounds. 4. 1,1,2-Triarylalkan-1-ols and 1,1,2-Triarylalk-1-enes containing basic ether groups, J. Med. Chem. 14 (1971) 952–957.
[26] R. McCague, G. Leclercq, N. Legros, J. Goodman, G.M. Blackburn, M. Jarman, A.B. Foster, Derivatives of tamoxifen. Dependence of antiestrogenicity on the 4-substituent, J. Med. Chem. 32 (1989) 2527–2533.
[27] R.R. Reddel, L.C. Murphy, R.E. Hall, R.L. Sutherland, Differential sensitivity of human breast cancer cell lines to the growth-inhibitory effects of tamoxifen, Cancer Res. 45 (1985) 1525–1531.
[28] D.W. Koh, T.M. Dawson, V.L. Dawson, Mediation of cell death by poly (ADP-ribose) polymerase-1, Pharmacol. Res. 52 (2005) 5–14.
[29] C.L. Fattman, B. An, L. Sussman, Q.P. Dou, p53-independent dephosphorylation and cleavage of retinoblastoma protein during tamoxifen-induced apoptosis in human breast carcinoma cells, Cancer Lett. 130 (1998) 103–113.
[30] S. Haldar, M. Negrini, M. Monne, S. Sabbioni, C.M. Croce, Down-regulation of bcl-2 by p53 in breast cancer cells, Cancer Res. 54 (1994) 2095–2097.
[31] K.H. Vousden, p53: death star, Cell 103 (2000) 691–694.
[32] E. Turpin, I. Bieche, P. Bertheau, L.-F. Plassa, F. Lerebours, A. de Roquancourt, M. Olivi, M. Espie, M. Marty, R. Lidereau, Increased incidence of ERBB2 overexpression and TP53 mutation in inflammatory breast cancer, Oncogene 21 (2002) 7593–7597.
[33] G.-J. Zhang, I. Kimijima, M. Onda, M. Kanno, H. Sato, T. Watanabe, A. Tsuchiya, R. Abe, S. Takenoshita, Tamoxifen-induced apoptosis in breast cancer cells relates to down-regulation of bcl-2, but not bax and bcl-XL, without alteration of p53 protein levels, Clin. Cancer Res. 5 (1999) 2971–2977.
[34] S.T. Bailey, H. Shin, T. Westerling, X.S. Liu, M. Brown, Estrogen receptor prevents p53-dependent apoptosis in breast cancer, Proc. Natl. Acad. Sci. 109 (2012) 18060–18065.
[35] A. Strasser, S. Cory, J.M. Adams, Deciphering the rules of programmed cell death to improve therapy of cancer and other diseases, Embo J. 30 (2011) 3667–3683.
[36] H. Yin, Q. Zhu, M. Liu, G. Tu, Q. Li, J. Yuan, S. Wen, G. Yang, GPER promotes tamoxifen-resistance in ER+ breast cancer cells by reduced Bim proteins through MAPK/Erk-TRIM2 signaling axis, Int. J. Oncol. 51 (2017) 1191–1198.
[37] A.R. Gomes, F. Zhao, E.W. Lam, Role and regulation of the forkhead transcription factors FOXO3a and FOXM1 in carcinogenesis and drug resistance, Chinese J. Cancer 32 (2013) 365–370.
[38] I.R. Hardcastle, M.N. Horton, M.R. Osborne, A. Hewer, M. Jarman, D.H. Phillips, Synthesis and DNA reactivity of α-hydroxylated metabolites of nonsteroidal antiestrogens, Chem. Res. Toxicol. 11 (1998) 369–374.
[39] L. Dasaradhi, S. Shibutani, Identification of tamoxifen-DNA adducts formed by α-sulfate tamoxifen and α-acetoxytamoxifen, Chem. Res. Toxicol. 10 (1997) 189–196.
[40] S.S. Dehal, D. Kupfer, Cytochrome P-450 3A and 2D6 catalyze orthohydroxylation of 4-hydroxytamoxifen and 3-hydroxytamoxifen (droloxifene) yielding tamoxifen catechol: involvement of catechols in covalent binding to hepatic proteins, Drug Metab. Dispos. 27 (1999) 681–688.
[41] M.M. Marques, F.A. Beland, Identification of tamoxifen-DNA adducts formed by 4-hydroxytamoxifen quinone methide, Carcinogenesis 18 (1997) 1949–1954.
[42] I.N. White, F. de Matteis, A. Davies, L.L. Smith, C. Crofton-Sleigh, S. Venitt, A. Hewer, D.H. Phillips, Genotoxic potential of tamoxifen and analogues in female Fischer F344/n rats, DBA/2 and C57BL/6 mice and in human MCL-5 cells, Carcinogenesis 13 (1992) 2197–2203.
[43] J. Styles, A. Davies, C. Lim, F. De Matteis, L. Stanley, I. White, Z.-X. Yuan, L. Smith, Genotoxicity of tamoxifen epoxide and toremifene in human lymphoblastoid cells containing human cytochrome P450s, Carcinogenesis 15 (1994) 5–9.
[44] Y. Ashida, A. Honda, Y. Sato, H. Nakatsuji, Y. Tanabe, Divergent synthetic access to E- and Z-stereodefined all-carbon-substituted olefin scaffolds: application to parallel synthesis of (E)- and (Z)-tamoxifens, Chemistryopen 6 (2017) 73–89.
[45] P. Germain, G. Harbrioux, Modulation of the estradiol-17 beta mitogenic effect on human breast cancer MCF-7 cells by serum albumin in defined medium, Anticancer Res. 13 (1992) 1581–1585.